Original research article

EJO European Journal of Ophthalmology

OCT-A evaluation of radiation vasculopathy following slotted plaque brachytherapy

European Journal of Ophthalmology
1–10

DOI: 10.1177/11206721211044339
journals.sagepub.com/home/ejo
SAGE

Anthony Fam, Ankit S Tomar and Paul T Finger

Abstract

Purpose: To determine a reliable diagnostic method to reveal and monitor subclinical progression of neural and perineural radiation vasculopathy.

Methods: A retrospective cross-sectional study, where optical coherence tomography angiography (OCT-A) imaging data was collected and analyzed from 22 consecutive patients that had been treated with circumneural slotted plaque brachytherapy for peripapillary, juxtapapillary, or circumpapillary choroidal melanomas. Pre-operative dosimetry of palladium-103 radiation dose to the optic nerve and fovea were collected. Quantified differences in OCT-A-measured vessel density and length in treated verses untreated contralateral control eyes were collected. Vessel density and length were correlated to radiation dose, plaque slot depth, visual acuity outcomes, and circumpapillary retinal nerve fiber layer thickness.

Results: Patients had post-irradiation follow-up of median 39 months, interquartile range 62 months). The mean optic disc radiation dose was 89.9 Gy $\pm$ 39.2 (86.5, 30.8–189.0). In comparison to controls, OCT-A imaging revealed significant differences in radial peripapillary capillary vessel density (18 μm^2 in case eyes, 34 μm^2 in control eyes; $p < 0.001$) and length (10 μm in case eyes, 14 μm in control eyes; $p < 0.001$). Change in vessel density did not show a significant correlation to radiation dose, slot depth, or visual acuity. However, change in vessel length was significantly correlated to radiation dose ($p = 0.049$) and change in visual acuity ($p < 0.001$).

Conclusions: OCT-A imaging revealed that radial peripapillary capillary vessel density and length were significantly reduced after circumneural irradiation for choroidal melanoma. Therefore, OCT-A imaging can be used to monitor progression of papillary vasculopathy associated with radiation optic neuropathy.

Keywords

OCT-A, choroidal melanoma, circumpapillary, plaque brachytherapy

Date received: 9 February 2021; accepted: 7 August 2021

Introduction

Optical coherence tomography angiography (OCT-A) has been found to be a non-invasive 3-D imaging modality that allows segmental vascular imaging of all retinal layers.[1,2] Signal decorrelation algorithms detect red blood cell flow, resulting in computerized high-resolution angiographic image reconstructions of the retinal capillary microcirculation.[1,2] OCT-A images have been quantitatively analyzed with consistent reproducibility.[3] Unlike fluorescein angiography, OCT-A does not require an injection of dye and yields computerized images amenable to segmentation and quantification. OCT-A offers a unique ability to image the deep capillary plexuses of the eye.[1,4]

Radiation vasculopathy has been the most common cause of severe irreversible blindness after ophthalmic radiation therapy.[5] After treatment, radiation causes a progressive vasculitis characterized by the loss of pericytes and endothelial cells. Early loss of vascular pericytes leads to exudation of intravascular components (serum, red blood cells and lipids). Exudation of serum leads to early vision loss due to edema. This is followed by the appearance of retinal hemorrhages and later cotton wool spots. The latter are evidence of endothelial cell loss associated vascular occlusions, perivascular ischemia, and

The New York Eye Cancer Center, New York, NY, USA

Corresponding author:
Paul T Finger, The New York Eye Cancer Center, Fifth Floor, 115 East 61st Street, New York, NY 10065, USA.
Email: pfinger@eyecancer.com

downstream tissue necrosis.[6] End-stage radiation retinopathy and optic neuropathy appear as capillary drop-out and optic disc pallor. Radiation vasculopathy has been shown to be dose and dose-rate dependent.[5]

Slotted plaque brachytherapy is circumneural. Therefore, it uniquely places the anterior optic nerve sheath and nerve disc as well as the short posterior ciliary vascular system within the irradiated zone. These treatments offer a unique opportunity to study radiation-induced papillary and peripapillary vasculopathy.[7–10]

Radiation optic neuropathy (RON) typically results in profound irreversible vision loss due to direct radiation-mediated vascular injury with early edema, followed by ischemia and axon loss. This study utilizes OCT-A to reveal vasculopathy of the radial peripapillary capillary (RPC) layers not previously seen with color photography, fluorescein angiography or OCT.[1,8–10]

Materials and methods

This was a retrospective cross-sectional study approved by Institutional Review Board and Ethics Committee of The New York Eye Cancer Center. The study was conducted in adherence with the Tenets of the Declaration of Helsinki and United States of America Health Insurance Portability and Accountability Act (HIPAA) of 1996.

Patient selection

OCT-A imaging was performed on eyes with peripapillary (within 1.5 mm of the optic disc), juxtapapillary (touching less than 180° of the optic disc) or circumpapillary (touching greater than 180°, and thus encircling the optic disc) choroidal melanomas. Their proximity to the optic nerve sheath-disc complex required the use of slotted plaque therapy to achieve American Brachytherapy Society (ABS) defined normal plaque positioning (Figure 1).[11] Each patient was diagnosed at The New York Eye Cancer Center between 2005 and 2019 and informed that the slotted gold-plaque would incorporate the optic nerve sheath complex and thus increase the risk for radiation optic neuropathy.[12] They were informed of our 12-year data on local control and visual acuity retention rates and that RON has been treatable with anti-vascular endothelial growth factor (anti-VEGF) therapy.[13–15] Lastly, patients with pre-existing optic neuropathy (including glaucoma) in either eye prior to plaque brachytherapy were excluded from this study.

Patient characteristics collected include age, sex, eye, and medical history (Table 1). Ophthalmic examinations included Early Treatment Diabetic Retinopathy Study ETDRS chart visual acuity measurements, intraocular pressure, and anterior segment examination. Tumor characteristics collected included tumor height and basal dimensions. Radiation parameters included in Table 2 were: plaque size, slot size (width and depth), tumor dose, tumor dose rate, hours of radiation exposure, and dose to critical ocular structures (fovea, optic disc, and sclera).

Medical physics

An explanation of the physical geometry of slotted plaques, the optic nerve and disc are important to understand slotted-plaque position during treatment.

Plaque slot width. The mean optic disc diameter is 1.8 mm. However, the retrobulbar optic nerve sheath diameter is 5.0–6.0 mm.[16] Therefore, standard round plaques placed against the retrobulbar optic nerve sheath will have its posterior edge at least 1.5 mm from the proximal optic disc margin. In the past, 4.0-mm wide notches were created to erroneously circumnavigate the 1.8 mm optic disc. The use of round and slotted plaques have been found to lead to posterior displacement of their posterior edges called "plaque tilt" and thus inaccurate placement.[17] To allow the plaque to lay flat around tumors near, touching and surrounding the optic disc, Finger employed a plaque slot width of 8.0-mm to accommodate the 5.0–6.0-mm diameter optic nerve sheath. Slots allowed the plaque to circumnavigate the optic nerve sheath and thereby advance beyond the optic nerve sheath obstruction.[7,18]

Plaque slot depth. Though all slots were 8.0-mm-wide, they were variably deep.[7,18] Finger modulated slot depth based on calculations of how far the optic nerve sheath need be accommodated within the gold plaque as to allow ABS normal plaque position (as to cover the entire tumor plus 2.0–3.0-mm free-margin) as seen in Figure 1. Prior to implantation, the radioactive palladium-103 seeds had to be strategically affixed within the plaque (around the slot) in order to fill in the radiation field.[11,18,19]

Radiation plaque surgery

Radiation dose measurements to critical intraocular structures were performed prior to plaque insertion.[13] Slotted plaque surgery was similar to traditional plaque surgery for choroidal melanoma.[11,18] However, in order to more readily access the optic nerve, rectus and oblique muscles were commonly relocated.[20] Slotted plaques were inserted to straddle and thus circumnavigate the retrobulbar optic nerve sheath. Ultrasound imaging was used to validate correct plaque placement.[21,22]

OCT and OCT-A data acquisition

Circumpapillary retinal nerve fiber layer (cpRNFL) thickness measures were acquired using spectral domain OCT (Spectralis®, Heidelberg Engineering, Heidelberg, Germany), utilizing TruTrack® Active Eye Tracking

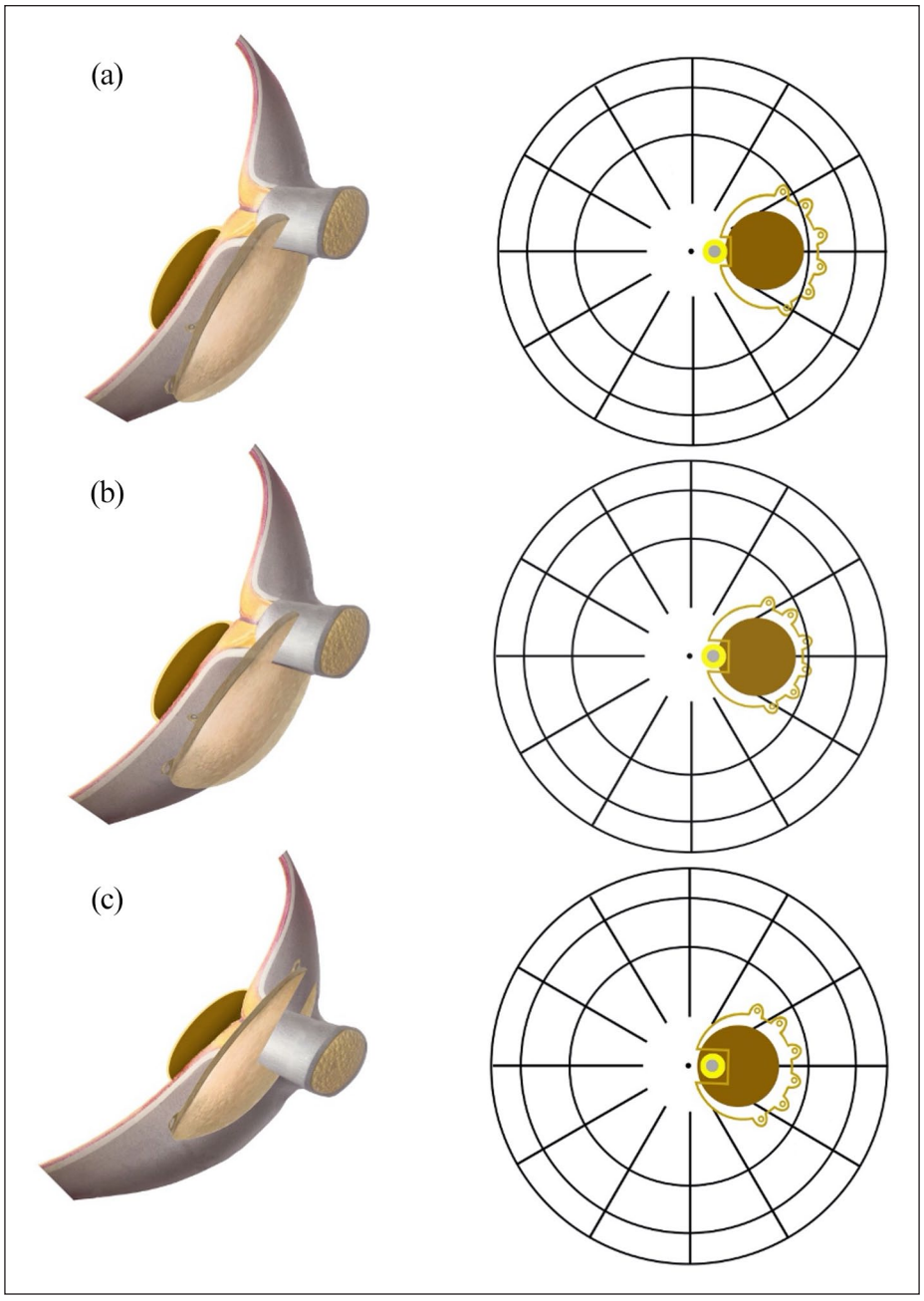

Figure 1. Slotted plaques relative to choroidal melanomas involving the optic nerve. Retinal drawings which show that variably slotted plaque depths can be used to deliver radiation to tumors involving the optic disc: (a) peripapillary choroidal melanoma, within 1.5 mm of the optic disc (b) juxtapapillary choroidal melanoma, touching less than 180° of the optic disc (c) circumpapillary choroidal melanoma, touching greater than 180°, and thus encircling the optic disc.
This figure first published in the American Journal of Ophthalmology, Vol. 188. Maheshwari A, Finger PT, "A 12-Year Study of Slotted Palladium-103 Plaque Radiation Therapy for Choroidal Melanoma: Near, Touching, Or Surrounding the Optic Nerve," pg. 60-69, Copyright Elsevier Inc. (2018) is reprinted with permission..

technology to reposition retina in real time when there was eye movement or blinking during the scan. This allows the operator to center the 3.5–3.6-mm diameter circle scan over the optic disc. Then, 768 equally spaced A-scans were produced, and cpRNFL thickness measurements from the four anatomic quadrants, along with the global average, was recorded. Quality of the scans, which used automatic real-time score, were included at minimum of 25 decibels.

OCT-A was performed using a Spectralis® OCT-A instrument. Spectral domain OCT settings were employed at a $10° \times 10°$ scan pattern with a resolution of 5.7 µm/pixel (512 A-scans × 512 B-scans). The system's native software identified temporal changes in the OCT signal (associated with red blood cell flow) in order to yield a map of perfused blood vessels in the retina (Figure 2, left).

Table 1. Patient demographics and tumor features.

Patient demographics and information	
Enrolled patients	22
Age; mean ± SD (median, range); years	68 ± 13 (71, 31–88)
Follow-up duration after plaque therapy; mean ± SD (median, range); months	64 ± 68 (39, 3–247)
Gender; *n* (%)	
Male	12 (54.5)
Female	10 (45.5)
Race; *n* (%)	
Caucasian	19 (86.4)
Hispanic	3 (13.6)
Significant past medical history; *n* (%)	
Hypertension	9 (40.9)
Diabetes	2 (9.1)
Prior cardiac illness	2 (9.1)
Tumor location: *n* (%)	
Superior	2 (9.1)
Superonasal	4 (18.2)
Nasal	6 (27.3)
Inferonasal	3 (13.6)
Inferior	2 (9.1)
Temporal	3 (13.6)
Superotemporal	2 (9.1)
Tumor features: mean ± SD (median, range); mm	
Tumor diameter	10.6 ± 3.0 (10.4, 5.9–16.0)
Tumor thickness	3.2 ± 1.7 (2.8, 1.30–7.90)
Distance to fovea	3.2 ± 2.3 (2.9, 0.0–7.2)
Distance to optic disc	0.3 ± 0.8 (0.0, 0.0–1.4)
Degree which optic disc is surrounded; degrees	168 ± 128 (180, 0–360)
Optic disc involvement: *n* (%)	
Peripapillary tumors	6 (27.3)
Juxtapapillary tumors	10 (45.5)
Circumpapillary tumors	6 (27.3)

SD: standard deviation; mm: millimeters; n: number of patients.

Images selected for analysis were acquired from the RPC segment, which extends from the upper boundary of the inner limiting membrane to the lower boundary of the RNFL. Peripapillary OCT-A blood vessel measurements have been found to be similar between individual patient eyes. Prior OCT-A studies have demonstrated that the contralateral eye can serve as a control when choroidal melanomas involve the optic nerve prior to radiation.[23,24] Therefore, differences in measurements between eyes have been interpreted as change resulting from irradiation.[24,25] The patients' contralateral eyes were used as a control for OCT-A RPC network scans.

The OCT-A en face slab was included following evaluation for the absence of motion artifact and for quality index >25 dB. Automated segmentation of the retinal layers was manually corrected when necessary.

Image analysis

Prior to exportation for image analysis, the area of the optic disc, as well as that of large arterioles and venules, were automatically subtracted from the en face image. Then, OCT-A images were exported for quantitative analysis using the open-source ImageJ software (National Institutes of Health, Bethesda, MD, USA). OCT-A image thresholding was performed using the Otsu algorithm, which performs a two cluster-based binarization in order to minimize intra-class variance and maximize inter-class variance (Figure 2, middle).[26] This Otsu method of thresholding was selected for its notable lack of bias in binarization particularly of the RPC layer, in comparison to other algorithms.[26] The area fraction measurement was used to calculate the vessel area density (VAD). Then the binarized image was skeletonized to reduce the thickness of every vessel to a single-pixel line, in order to determine the ratio of the image occupied by the vessels, irrespective of vessel diameter. The vessel length fraction (VLF) was calculated using the area fraction measurement feature (Figure 2, right). VLF is a useful parameter included to measure the inter-eye differences in retinal microvasculature that is not attributable to differences in vessel lumen size.

Table 2. Dosimetry, plaque parameters, and imaging features post-radiation therapy.

Plaque parameters: mean ± SD (median, range); size in mm			
Plaque diameter size		16 ± 2 (16, 12–20)	
Depth of plaque slot		4 ± 2 (4, 1.0–6.5)	
Radiation dose to ocular structures: mean ± SD (median, range); Dose in Gy			
Tumor apex		87 ± 18 (85, 70–160)	
Sclera		200.7 ± 83 (175.8, 113.8–449.5)	
Fovea		70.9 ± 58.0 (62.7, 11.7–212.9)	
Optic disc		89.9 ± 39.2 (86.5, 30.8–189.0)	
Optic disc treated with plaque depth <4 mm		78.6 ± 27.0 (86.5, 30.8–115.5)	
Optic disc treated with plaque depth ⩾4 mm		99.4 ± 41.7 (86.0, 37.5–189.0)	
Radiation dose rate to ocular structures: mean ± SD (median, range); Dose rate in Gy/h			
Tumor apex		44.3 ± 33.7 (33.1, 12.8–168.5)	
Sclera		117.1 ± 73.8 (107.9, 14.0–312.8)	
Fovea		49.7 ± 41.5 (42.1, 8.1–145.3)	
Optic disc		58.5 ± 24.2 (57.5, 21.4–109.1)	
	At presentation	At follow-up	*p*
Visual acuity: mean ± SD (median, range)			
Snellen	20/30	20/50	0.060
logMAR	0.2 ± 0.3 (0.0, 0.0–0.8)	0.4 ± 0.6 (0.1, 0.0–2.2)	0.060
	Control eye	Irradiated eye	*p*
OCT cpRNFL thickness: mean ± SD (median, range)			
Global average	96 ± 9 (96, 82–112)	102 ± 18 (100, 70–134)	0.448
OCT-A RPC vessel average density: mean ± SD (median, range)			
en face	34 ± 11 (34, 10–58)	18 ± 12 (17, 2–46)	**<0.001**
OCT-A RPC vessel length fraction: mean ± SD (median, range)			
en face	14 ± 2 (14, 9–17)	10 ± 3 (11, 4–17)	**<0.001**

SD: standard deviation; mm: millimeter; OCT-A: optical coherence tomography angiography; Gy: Gray (radiation dose); cpRNFL: circumpapillary retinal nerve fiber layer; RPC, retinal peripapillary capillaries.
Boldface: $p < 0.05$.

Statistical analysis

Continuous variables were described using median, mean, and range. Categorical variables were described using frequencies and proportions. Student's *t*-test for paired data was used for VAD, VLF, visual acuity, and cpRNFL between the case and control eyes. The relationship between continuous parameters were assessed by means of Pearson's correlation coefficient. The Mann–Whitney *U* test was used for the analysis of nonparametric data which was not normally distributed. Statistical significance was set at $p < 0.05$. All statistical analysis was performed using a statistical software package (SPSS version 26.0, IBM, Armonk, New York, USA).

Results

We reviewed 61cases of patients treated with palladium-103 slotted plaque brachytherapy. However, within the past 14 months, OCT-A imaging was available for 26 consecutive patients who had returned for follow-up and had sufficiently clear media for examination. Of these, OCT-A artifacts prevented four patients from being included in the study. The remaining 22 patients had a mean age of 68 years ±13 (median 71, range 31–88). The majority were male (12/22, 54.5%) and Caucasian (19/22, 86.4%). Features of the patients' choroidal melanomas (size, distance to optic nerve, and degree of surrounding the optic nerve) are summarized in Table 1. Radiation parameters and calculated doses to the tumor and critical intraocular structures can be found in Table 2. OCT-A scans were obtained at a median follow-up time of 39 months (interquartile range 62 months) after slotted plaque radiation therapy. OCT-A quality index for control eyes had an average of 34 ± 3 (median 34, range 28–39), while case eyes had an average of 33 ± 3 (median 33, range 29–39). There was no significant difference between the quality of the scans of case and control eyes ($p = 0.274$).

Visual acuity

Of the 22 patients, follow-up after radiotherapy was a mean 64 months ±68 (median 39, range 3–247). The LogMAR

visual acuity of both of each patient's eyes were comparable prior to radiation therapy, with a mean 0.2 ± 0.3 (median 0.0, range 0.0–0.8) or Snellen chart equivalent of 20/32. At the latest follow-up, the average logMAR visual acuity was 0.4 ± 0.6 (median 0.1, range 0.0–2.2) or Snellen chart equivalent of 20/50. The decrease in visual acuity was not significant ($p = 0.060$) and 18 eyes (81.8%) did not lose more than three lines of vision.

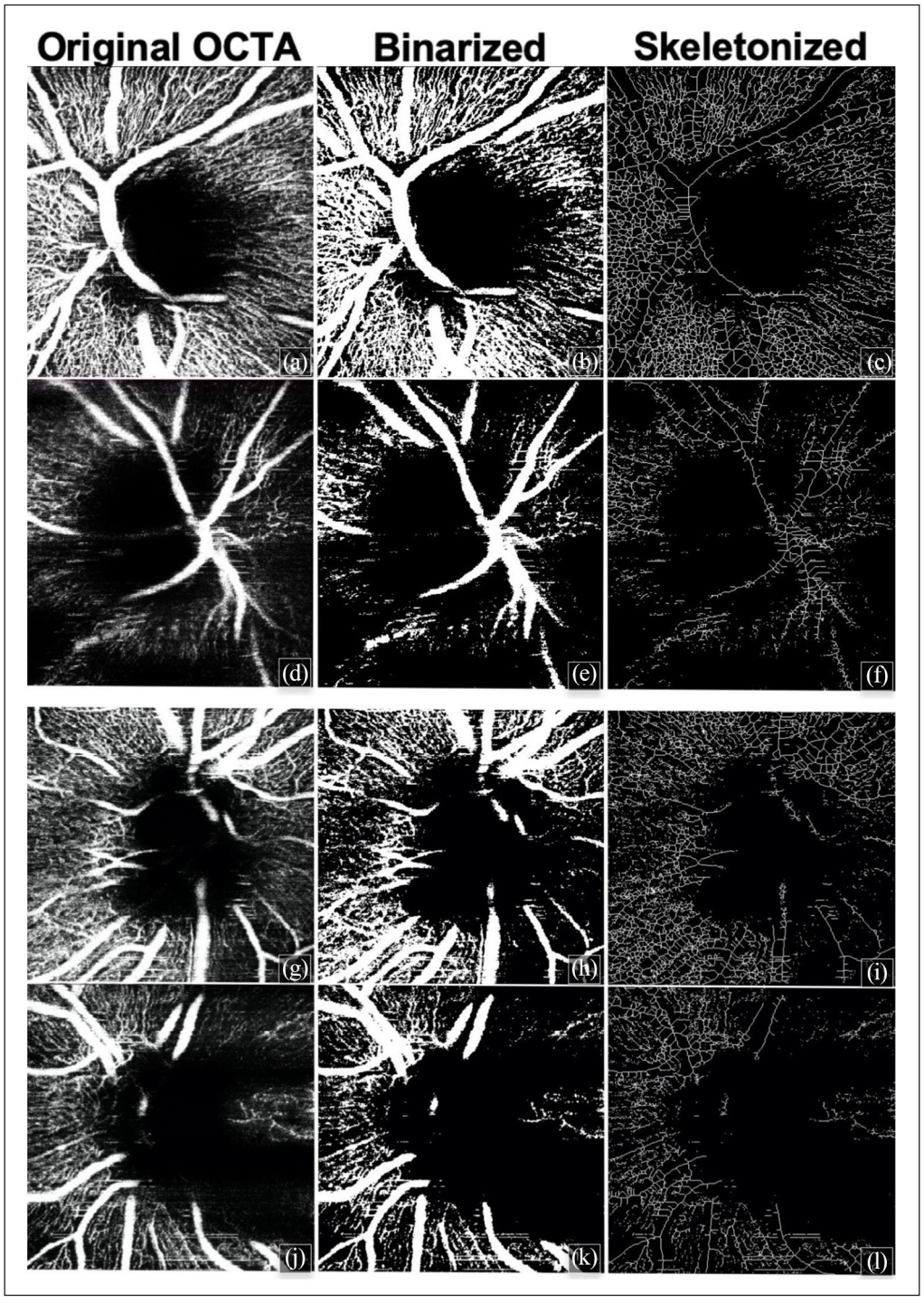

Figure 2. *(Continued)*

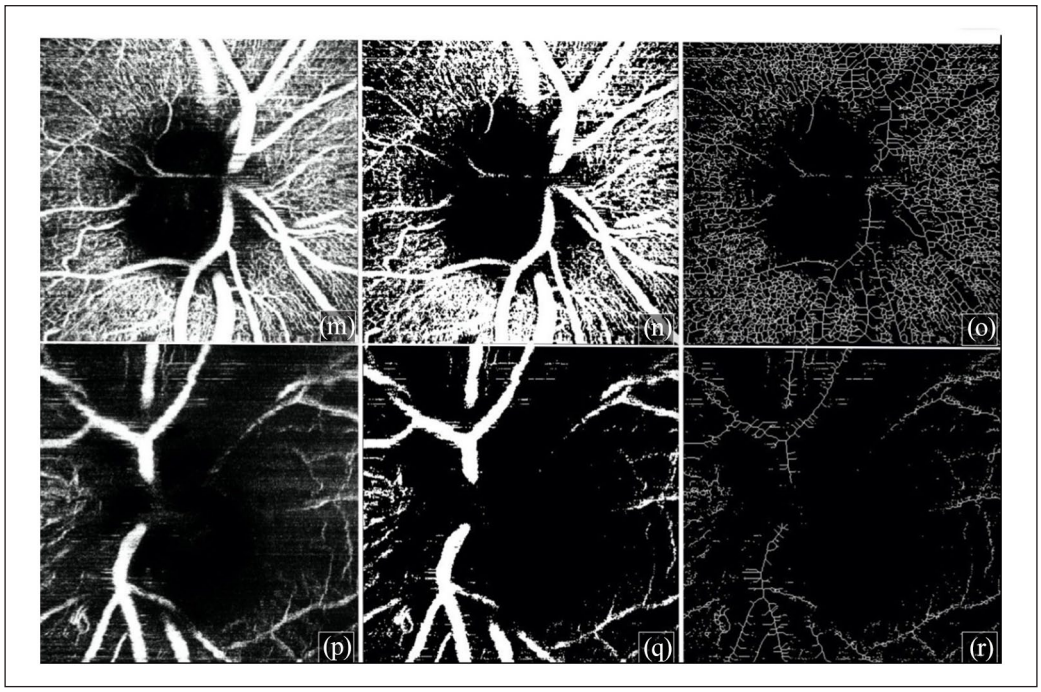

Figure 2. OCT-A on acquisition and processing for vessel density and length measures. Optical coherence tomography angiography was obtained for all treated case eyes and contralateral control eyes. En face images, presented in the left column, are unfiltered images from acquisition. These were then binarized into the images in the middle column, to be used for vessel density calculation. Finally, binarized images were skeletonized into the images in the right column, to be used for vessel length calculation. Patient 1 (a–f): control eye scans shown in (a–c), and case eye scans shown in (d–f). Patient 2 (g–l): control eye scans shown in (g–i), and case eye scans shown in (j–l). Patient 3 (m–r): control eye scans shown in (m–o), and case eye scans shown in (p–r).

OCT retinal nerve fiber layer changes

OCT and OCT-A data from treated and control eyes is shown (Table 2). cpRNFL was measured in 10 of the 22 patients by OCT. The cpRNFL of the case eyes had a mean of $102\,\mu m \pm 18$ (median 100, range 70–134), while the control eye had a mean cpRNFL of $96\,\mu m \pm 9$ (median 96, range 82–112). There was no significant difference ($p = 0.448$).

OCT-A vessel average density changes

The mean case RPC VAD en face was $18\,\mu m^2 \pm 12$ (median 17, range 2–46), and in the control eye was $34\,\mu m^2 \pm 11$ (median 34, range 10–58). This was a significant reduction in the RPCVAD compared to control ($p < 0.001$).

OCT-A vessel length fraction changes

The mean case RPC VLF en face was $10\,\mu m \pm 3$ (median 11, range 4–17), and in the control eye was $14\,\mu m \pm 2$ (median 14, range 9–17). This was also a significant reduction in the RPC VLF compared to control ($p < 0.001$).

Plaque slot depth effects

Plaque slot depth governs how much of the optic nerve is accommodated within the plaque during radiation therapy. For example, a 4.0-mm slot will accommodate approximately two-thirds of the retrobulbar optic nerve sheath and thus allow the posterior edge of a slotted plaque to typically reach 1 mm beyond the contralateral edge of the optic disk. Eyes treated with a plaque slot depth less than 4.0-mm (10 of 22 patients) had a mean optic disc radiation dose of $78.6\,Gy \pm 27.0$ (86.5, 30.8–115.5), while those with plaque slot depths of 4.0-mm or more (12 of 22 patients) had a mean optic disc radiation dose of $99.4\,Gy \pm 41.7$ (86.0, 37.5–189.0). Comparison of these groups revealed no significant difference in the change in VAD ($p = 0.346$), VLF ($p = 0.238$) or visual acuity ($p = 0.539$) (Table 3).

OCT-A clinical correlations

The data on radiation dose, visual acuity, plaque slot depth, VAD, VLF, and mean follow-up is shown in Table 3. Note that there were no significant correlations associated with the change in VAD en face. However, there was a significant correlation between the change in en face VLF in comparison to the radiation dose to the optic disc

Table 3. Correlations of clinical, radiation, and imaging parameters.

	r		*p*
Change in vessel average density en face			
Radiation dose to optic disc	0.314		0.177
Radiation dose rate to optic disc	0.324		0.163
Change in visual acuity	0.418		0.053
Change in vessel length fraction en face			
Radiation dose to optic disc	0.446		**0.049**
Radiation dose rate to optic disc	0.430		0.059
Change in visual acuity	0.727		**<0.001**
	Group 1	**Group 2**	***p***
Plaque slot depth: mean ± SD (median, range)	<4 mm depth	⩾4 mm depth	
Number of patients	10	12	
Change in VAD en face	14 ± 13 (11, −6 to 35)	18 ± 8 (16, 7 to 31)	0.346
Change in VLF en face	2 ± 3 (2, −1 to 7)	4 ± 4 (4, −1 to 11)	0.238
Drop in visual acuity lines	1.1 ± 2.5 (0.0, 0.0 to 8.0)	3.1 ± 6.6 (0.5, −1.0 to 16.0)	0.539

SD: standard deviation; VAD: vessel average density; VLF: vessel length fraction.
Boldface: $p < 0.05$.

($p = 0.049$). Likewise, although the reduction in visual acuity was not significant, the correlation between the change in VLF and the trend of reduction in visual acuity was significant ($p < 0.001$).

Discussion

This study demonstrated that at a mean 64 months after slotted-plaque radiation therapy, there was no significant difference in cpRNFL thickness on OCT compared to the contralateral eye. However, there were significant reductions in OCT-A-measured VADs and VLFs in irradiated eyes. Finally, 81.8% of patients maintained within three lines of vision at last follow-up. Reductions in VAD and VLF of the RPC vessels may therefore precede OCT and clinical manifestations of radiation vasculopathy.

Increasing radiation dose to the optic disc was correlated with reductions in VLF in the RPC plexus ($p = 0.049$), suggesting that higher doses of radiation to the optic nerve results in a greater reduction in peripapillary capillary vasculature. These reductions in VLF were correlated with a trend of reduction in visual acuity ($r = 0.727$, $p < 0.001$), while reductions in VAD were not. Though visual acuity did not decrease significantly in this cohort, the correlation with VLF and visual acuity suggests that VLF may be found to be a useful parameter in predicting the onset of significant radiation-related vision loss prior to its occurrence. It is possible that VADs may be falsely increased because radiation-induced ischemia of smaller capillaries results in dilation of larger upstream vessels, increasing the vessels' pixel density.[27] However, since the skeletonization algorithm used in VLF reduces all vessel diameters to a single pixel, it suggests that VLF was not affected by vessel dilation.

Comparative literature

Given the recent advent of OCT-A imaging, only a small number of studies were found to utilize OCT-A in the evaluation of the RPC plexus.[23,24,28,29] Two studies examined a combined 20 patients after plaque therapy near the optic disc.[23,24] Both found a reduction of RPC-VAD in OCT-A as a subclinical manifestation of RON. However, patient treatments were performed with round or notched plaques. These plaque designs force an offset of the radiation zone away from the optic disc, relying on "plaque-tilt and spray" to dose the posterior edges of peripapillary melanomas and induce radiation dose uncertainty.[22] Geographic plaque mis-alignment and radiation dose inaccuracy not only results in higher rates of treatment failure, but confounds observations of dosimetric effects on OCT-A measured vessel change.[11,17,30] For example, utilizing round and notched plaques as well as case selection, Sagoo et al. achieved 75% local tumor control. In contrast, with Finger's slotted plaques in treatment of consecutive patients with peripapillary, juxtapapillary and circumpapillary melanomas, Maheshwari and Finger[18,31] reported 98.2% local control. They found that accommodating the optic nerve sheath complex seats the plaque as to cover the entire tumor and free margin. It eliminates "tilt and spray" in favor of an ABS-normal, quantifiable radiation field, evidenced by superior local control rates.

Slotted plaque brachytherapy offered an accurate interpretation of plaque radiation dose effects on RPC vessel density and length.[18,23,24,30,31] Like other studies, we found that radiation-induced vasculopathy occurred at the RPC plexus, a layer which only OCT-A can image.[4,29,32] However, our study differed in that a more accurately, quantified radiation dose to the optic disc was

recorded, due to the virtual elimination of tilt and spray as seen with unslotted plaques. Finally, our study agrees with Parrozzani et al.,[28] in that we also found that the VLF parameter was more sensitive to perfusion changes at the capillary level and could be used to correct for bias in the VAD measurement.

Weaknesses

Our study design included patients who had been treated prior to the advent of OCT-A. Prospective studies will better elucidate the relationship between changes in VAD and VLF as well as visual acuity over time. Such studies will also allow for a regression analysis correlating OCT-A measurements to subclinical and clinical stages of RON. Finally, the study included 22 patients in total, only 10 of whom had cpRNFL data. This relatively small number of patients is due to the rarity of the location of the tumors which were analyzed.

Strengths

This study examines vascular effects related to well-quantified plaque irradiation dose to the optic nerve. In order to achieve this analysis, we utilize a relatively unique subset of peripapillary, juxtapapillary, and circumpapillary choroidal melanomas treated with slotted eye plaques. All surgeries were performed by a single ocular oncologist (PTF) who invented, employed and has published long-term clinical outcomes after slotted plaque brachytherapy for peripapillary, juxtapapillary, and circumpapillary choroidal melanoma.[7,11,33–35]

Conclusions

Though the retina and optic nerve may appear healthy after irradiation, the micro-vasculature of the RPC plexus can be monitored with OCT-A imaging. Our study revealed that VLF measurements can be used to detect subclinical manifestations of RON. This offers the potential to use this information to modulate by anti-VEGF therapy to preserve vision.[15] OCT-A has revealed what we could not see before and offers a better understanding of vasculopathy related to radiation optic neuropathy.

Acknowledgements

All authors had full access to all of the data in the study and take responsibility for the integrity of the data and the accuracy of the data analysis, which is available upon reasonable request. All authors have no conflicts of interest involving the work under consideration for publication, relevant financial activities outside the submitted work, nor other relationships or activities that readers could perceive to have influenced, or that give the appearances of potentially influencing this submitted work.

Declaration of conflicting interests

The author(s) declared no potential conflicts of interest with respect to the research, authorship, and/or publication of this article.

Funding

The author(s) disclosed receipt of the following financial support for the research, authorship, and/or publication of this article: This work was supported by an unrestricted grant from The Eye Cancer Foundation, Inc., (http://eyecancercure.com). Dr. Ankit Singh Tomar received a Fellowship Grant from The Eye Cancer Foundation to study Ocular Tumor, Orbital Disease and Ophthalmic Radiation Therapy with Dr. Finger.

ORCID iD

Paul T Finger https://orcid.org/0000-0002-8111-3896

References

1. Akil H, Falavarjani KG, Sadda SR, et al. Optical coherence tomography angiography of the optic disc; an overview. *J Ophthalmic Vis Res* 2017; 12(1): 98–105.
2. de Carlo TE, Romano A, Waheed NK, et al. A review of optical coherence tomography angiography (OCTA). *Int J Retina Vitreous* 2015; 1: 5.
3. Chen CL, Bojikian KD, Xin C, et al. Repeatability and reproducibility of optic nerve head perfusion measurements using optical coherence tomography angiography. *J Biomed Opt* 2016; 21(6): 65002.
4. Keane PA and Sadda SR. Retinal imaging in the twenty-first century: state of the art and future directions. *Ophthalmology* 2014; 121(12): 2489–2500.
5. Finger PT. Radiation therapy for orbital tumors: concepts, current use, and ophthalmic radiation side effects. *Surv Ophthalmol* 2009; 54(5): 545–568.
6. Archer DB, Amoaku WM and Gardiner TA. Radiation retinopathy–clinical, histopathological, ultrastructural and experimental correlations. *Eye (Lond)* 1991; 5(Pt 2): 239–251.
7. Finger PT. Finger's "slotted" eye plaque for radiation therapy: treatment of juxtapapillary and circumpapillary intraocular tumours. *Br J Ophthalmol* 2007; 91(7): 891–894.
8. Yousef YA and Finger PT. Optical coherence tomography of radiation optic neuropathy. *Ophthalmic Surg Lasers Imaging* 2012; 43(1): 6–12.
9. Behbehani R. Clinical approach to optic neuropathies. *Clin Ophthalmol* 2007; 1(3): 233–246.
10. Yang H, Wang W, Hu HL, et al. Clinical analysis of radiation optic neuropathy. *Zhonghua Yan Ke Za Zhi* 2011; 47(12): 1071–1075.
11. American Brachytherapy Society – Ophthalmic Oncology Task Force. The American Brachytherapy Society consensus guidelines for plaque brachytherapy of uveal melanoma and retinoblastoma. *Brachytherapy* 2014; 13(1): 1–14.
12. Danesh-Meyer HV. Radiation-induced optic neuropathy. *J Clin Neurosci* 2008; 15(2): 95–100.

13. Finger PT. Anti-VEGF bevacizumab (Avastin) for radiation optic neuropathy. *Am J Ophthalmol* 2007; 143(2): 335–338.
14. Finger PT and Mukkamala SK. Intravitreal anti-VEGF bevacizumab (Avastin) for external beam related radiation retinopathy. *Eur J Ophthalmol* 2011; 21(4): 446–451.
15. Finger PT, Chin KJ and Semenova EA. Intravitreal anti-VEGF therapy for macular radiation retinopathy: a 10-year study. *Eur J Ophthalmol* 2016; 26(1): 60–66.
16. Garcia JP Jr, Garcia PT, Rosen RB, et al. A 3-dimensional ultrasound C-scan imaging technique for optic nerve measurements. *Ophthalmology* 2004; 111(6): 1238–1243.
17. Almony A, Breit S, Zhao H, et al. Tilting of radioactive plaques after initial accurate placement for treatment of uveal melanoma. *Arch Ophthalmol* 2008; 126(1): 65–70.
18. Maheshwari A and Finger PT. A 12-year study of slotted Palladium-103 plaque radiation therapy for choroidal melanoma: near, touching, or surrounding the optic nerve. *Am J Ophthalmol* 2018; 188: 60–69.
19. Collaborative Ocular Melanoma Study Group, Diener-West M, Earle JD, Fine SL, et al. The COMS randomized trial of Iodine 125 brachytherapy for choroidal melanoma, III: initial mortality findings. COMS report no. 18. *Arch Ophthalmol* 2001; 119(7): 969–982.
20. Nagendran ST, Finger PT and Campolattaro BN. Extraocular muscle repositioning and diplopia: associated with ophthalmic plaque radiation therapy for choroidal melanoma. *Ophthalmology* 2014; 121(11): 2268–2274.
21. Finger PT, Romero JM, Rosen RB, et al. Three-dimensional ultrasonography of choroidal melanoma: localization of radioactive eye plaques. *Arch Ophthalmol* 1998; 116(3): 305–312.
22. Harbour JW, Murray TG, Byrne SF, et al. Intraoperative echographic localization of iodine 125 episcleral radioactive plaques for posterior uveal melanoma. *Retina* 1996; 16(2): 129–134.
23. Skalet AH, Liu L, Binder C, et al. Quantitative OCT angiography evaluation of peripapillary retinal circulation after plaque brachytherapy. *Ophthalmol Retina* 2018; 2(3): 244–250.
24. Chien JL, Sioufi K, Ferenczy SR, et al. Optical coherence tomography angiography detects subclinical radial peripapillary capillary density reduction after plaque radiotherapy for choroidal melanoma. *Retina* 2020; 40: 1774–1782.
25. Rao HL, Pradhan ZS, Weinreb RN, et al. Determinants of peripapillary and macular vessel densities measured by optical coherence tomography angiography in normal eyes. *J Glaucoma* 2017; 26(5): 491–497.
26. Rabiolo A, Gelormini F, Sacconi R, et al. Comparison of methods to quantify macular and peripapillary vessel density in optical coherence tomography angiography. *PLoS One* 2018; 13(10): e0205773.
27. Kim AY, Chu Z, Shahidzadeh A, et al. Quantifying microvascular density and morphology in diabetic retinopathy using spectral-domain optical coherence tomography angiography. *Investig Ophthalmol Vis Sci* 2016; 57(9): OCT362–OCT370.
28. Parrozzani R, Frizziero L, Londei D, et al. Peripapillary vascular changes in radiation optic neuropathy: an optical coherence tomography angiography grading. *Br J Ophthalmol* 2018; 102(9): 1238–1243.
29. Mase T, Ishibazawa A, Nagaoka T, et al. Radial peripapillary capillary network visualized using wide-field montage optical coherence tomography angiography. *Investig Ophthalmol Vis Sci* 2016; 57(9): OCT504–OCT510.
30. Jampol LM, Moy CS, Murray TG, et al. The COMS randomized trial of iodine 125 brachytherapy for choroidal melanoma: IV. Local treatment failure and enucleation in the first 5 years after brachytherapy. COMS report no. 19. *Ophthalmology* 2020; 127(4S): S148–S157.
31. Sagoo MS, Shields CL, Mashayekhi A, et al. Plaque radiotherapy for choroidal melanoma encircling the optic disc (circumpapillary choroidal melanoma). *Arch Ophthalmol* 2007; 125(9): 1202–1209.
32. Yu PK, Balaratnasingam C, Xu J, et al. Label-free density measurements of radial peripapillary capillaries in the human retina. *PLoS One* 2015; 10(8): e0135151.
33. Chiu-Tsao ST, Astrahan MA, Finger PT, et al. Dosimetry of 125 I and 103 Pd COMS eye plaques for intraocular tumors: report of Task Group 129 by the AAPM and ABS. *Med Phys* 2012; 39(10): 6161–6184.
34. Finger PT. Radiation therapy for choroidal melanoma. *Surv Ophthalmol* 1997; 42(3): 215–232.
35. Finger PT. Plaque brachytherapy for choroidal melanoma: strategies and techniques to reduce risk and maximize outcomes. *Expert Rev Ophthalmol* 2020; 15(4): 201–210.